Check for updates

Research Article
Open Access

MJ Cell Press

MJ Engineering Sciences

Available at: https://mjcellpress.com/article/mjes09/

MJ Engineering Sciences

Analysis of the Photovoltaic Solar Potential of the City of Boali in the Central African Republic for a Local Energy Transition

Igor Prince Martial Bondobo[1*], Cyrille Rodrigue Enone Ellah[1], Ahmed El-Kebir Iya[1], Noé Landry Privace M'bouana[2], Ruben Martin Mouangue[1]

[1] Laboratory of Energy, National Higher Polytechnic School of Douala, University of Douala, Cameroon.

[2] Higher Institute of Technology, University of Bangui, Central African Republic.

[*]Corresponding author: igorbondobo@yahoo.fr

Key words

Boali,
Electricity production,
Solar photovoltaic,
Solar irradiance,
Module temperature.

Abstract

Electrification in the Central African Republic (CAR) continues to represent a critical challenge to its socio-economic development, particularly in rural areas, where access to electricity remains below 3%. In this context, photovoltaic solar energy stands out as an especially promising alternative, given the country's considerable solar resource potential. The present study assesses the photovoltaic potential of Boali using hourly climatic data obtained from the SolarGIS and NASA POWER databases. The Skoplaki model was employed to estimate the operating temperature of the photovoltaic modules, which subsequently enabled the calculation of the expected electrical output of a 500 Wp solar panel. The results indicate that a single panel can generate approximately 28.3 kWh per year, a value comparable to the average annual per-capita electricity consumption in the CAR. These findings underscore the favorable climatic conditions of Boali for the implementation of solar-based electrification projects.

Received:10.09.2025 Accepted: 26.11.2025 Published online: 19.12.2025

How to cite this article: Bondobo, I. P. M., Enone Ellah, C. R., Iya, A. E.-K., M'Bouana, N. L. P., & Mouangue, R. M. (2025). (2025). *Analysis of the photovoltaic solar potential of the city of Boali in the Central African Republic for a local energy transition. MJ Engineering Sciences*. *1*(2), 127–143. https://doi.org/10.63156/mjes09

1. Introduction

In an article published in 2023, Olong et al. [1] examined the global energy transition and highlighted the central role of renewable energy sources in mitigating climate change. Their findings confirm that solar energy is among the most promising resources, as it is widely available, particularly in regions characterized by high levels of solar irradiance. This observation underscores the importance of addressing access to modern energy in Africa, which remains a crucial lever for poverty reduction and socio-economic development.

During the early 2010s, more than 600 million people across the African continent were estimated to be without access to electricity, while approximately 80 % of the population relied primarily on traditional biomass for cooking [2]. In the Central African Republic, several renewable energy options have been investigated, with particular

attention given to wind and solar resources. This assertion is supported by studies carried out by Ngbara et al., who assessed wind potential in the cities of Bangui and Bouar [3,4], as well as by more recent projects demonstrating the technical feasibility of large-scale solar power plants in the vicinity of Bangui.

On 27 March 2023, the Central African Republic officially inaugurated a 15 MWp photovoltaic power plant in Sakaï, located approximately 10 km south of the capital city, Bangui. This initiative was followed on 17 November 2023 by the commissioning of a 25 MWp solar farm in the village of Danzi, situated about 18 km from Bangui, with the capacity to supply electricity to nearly 250,000 inhabitants [5,6]. The second installation enabled the replacement of more than 90 % of the former diesel-based energy production with sustainable solar energy, resulting in a substantial reduction in carbon dioxide emissions, estimated at a cumulative net decrease of 670,674 tons [6].

Nevertheless, access to electricity continues to represent a significant challenge for the population. According to the World Bank's development indicators, only 17.6 % of the population had access to electricity in 2023, with a marked disparity between urban areas (37.4 %) and rural regions (2.3 %) [7]. Figure 1 illustrates the temporal fluctuations in the rate of electricity access in the Central African Republic. As reflected by these data, progress remains gradual with regard to the universal access objectives defined under the United Nations 2030 Agenda for Sustainable Development. The integration of energy generated by solar power plants into the existing distribution network has been shown to be technically feasible, as demonstrated by Fumtchum et al. [8] in their study on the injection efficiency of solar photovoltaic energy into the urban grid of Douala, Cameroon—a neighbouring country with a comparable energy access context. Such integration could contribute to a further improvement in national electrification rates.

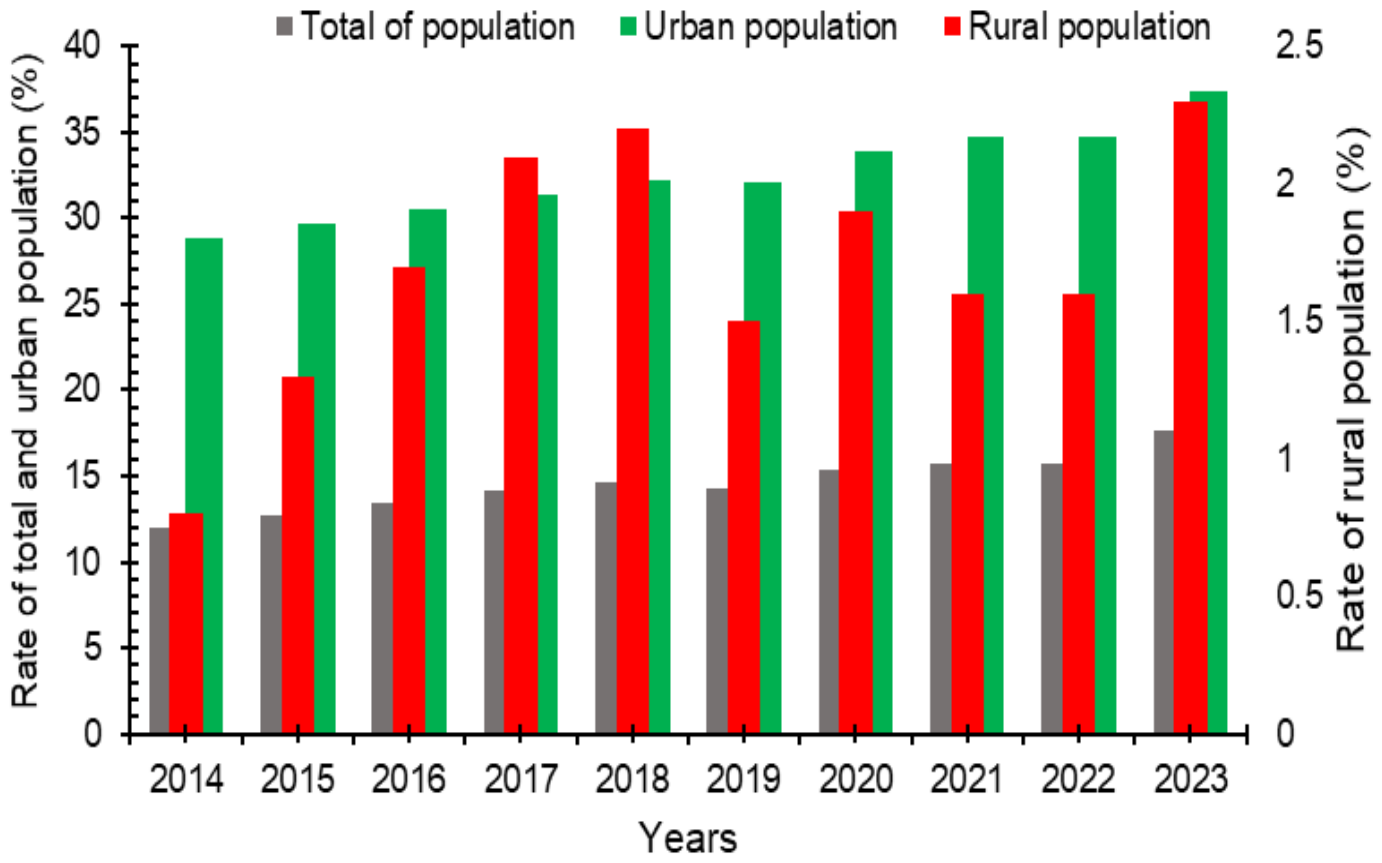

Figure 1 : Changes in the rate of access to electricity in CAR between 2014 and 2023 (Source: World Bank [7])

In addition to the solar power plants mentioned above, several other sites could be explored in order to increase the national rate of access to electricity. The objective of the present study is therefore to assess the photovoltaic solar

potential of the town of Boali. However, such an assessment requires the consideration of multiple meteorological parameters, all of which may significantly influence the efficiency of solar radiation conversion into electrical energy.

The existing literature clearly establishes a strong correlation between the operating temperature of photovoltaic cells and their energy yield. An increase in temperature has been shown to induce a significant decrease in open-circuit voltage, as well as a deterioration of the fill factor, thereby negatively affecting the overall performance of the system [9]. Numerous mathematical models have been developed to estimate this operating temperature, and these may be classified according to different scientific and methodological approaches.

Empirical models are based on simple statistical correlations between module temperature and environmental variables, including solar irradiance, ambient temperature and, in some cases, wind speed. Generally expressed in the form of equation (1), these models are characterized by their ease of calibration and rapid implementation. Their accuracy, however, is often limited to specific climatic conditions. The seminal contributions of Skoplaki et al. [10], Trinuruk et al. (2009) [11], Aoun [12,13] and Bailek et al. [14] exemplify this approach, with some of the proposed correlations being particularly adapted to arid or tropical environments.

$$T_m = T_a + \frac{G}{\alpha + \tau V} \quad (1)$$

where T_a is the ambient temperature, α\alphaα is the heat-loss coefficient in the absence of wind (W/m²·K), and τ\tauτ is the wind-related forced convection coefficient.

In addition, physically based models have been developed that rely on an energy balance of the photovoltaic module. These models incorporate heat transfer mechanisms through conduction, convection, and radiation. They require detailed knowledge of thermophysical parameters, such as absorptivity, emissivity, and system efficiency. Nonetheless, this approach offers greater generality and wider applicability. Studies conducted by Kaplani and Kaplanis [15], de Souza et al. [16], and Aly et al. [17] are consistent with this modelling framework. Such models also allow for the integration of the effects of installation geometry and wind conditions on heat transfer coefficients.

Subsequently, dynamic models have been introduced to account for temporal variations in temperature by incorporating the thermal inertia of photovoltaic modules. As illustrated in equation (2), such processes are commonly expressed using differential equations:

$$C\frac{T_m}{dt} = \alpha G - U(T_m - T_a) \quad (2)$$

Notable contributions in this domain include the works of Perović et al. [18], Barry et al. [19], and Frid et al. [20], which have proven to be particularly useful for real-time simulations or under highly variable operating conditions.

With the advent of Big Data and artificial intelligence, several authors have also proposed module temperature prediction models based on machine learning techniques. Artificial neural networks (Coskun et al. [21]; Serrano-Luján et al. [22]), random forests, and radial basis function (RBF) networks (Xiaojian et al. [23]) are capable of capturing the complex non-linear relationships between climatic variables and temperature. Many studies have further refined these models by adjusting heat transfer coefficients and boundary conditions. Significant contributions in this area include the works of Orazio et al. [24], Martín-Chivelet et al. [25], and Assoa et al. [26,27].

A review published by Santos et al. [28] identifies 33 distinct models for estimating the operating temperature of photovoltaic modules, together with the parameters considered in each case. These models are summarized in Table 1.

Table 1: Models for estimating the operating temperature of PV modules with the parameters taken into account [28].

Correlations vs parameters	G	T_a	V_w	η	α	τ	G_{NOCT}	$T_{c,NOCT}$	$T_{a,NOCT}$	β	U	Other inputs (appear in five or less of the studied correlations)
Fernández *et al.*	✓	×	✓	×	×	×	×	×	×	×	×	V_{oc}, c_1, c_2, c_3
Durisch *et al.*	✓	✓	×	×	×	×	×	×	×	×	×	k
Nordmann and Clavadetscher	✓	✓	×	×	×	×	×	×	×	×	×	k
Krauter	✓	✓	×	×	×	×	×	×	×	×	×	k
Mondol *et al.* I	✓	✓	×	×	×	×	×	×	×	×	×	
Hove	✓	✓	×	✓	✓	✓	×	×	×	×	✓	
Tiwari	✓	✓	×	✓	✓	✓	×	×	×	×	✓	
Eicker	✓	✓	×	✓	✓	×	×	×	×	×	✓	
Standard	✓	✓	×	×	×	×	✓	✓	✓	×	×	
Davis	✓	✓	×	✓	✓	✓	✓	✓	✓	×	×	
Mondol *et al.* II	✓	✓	×	×	×	×	×	×	×	×	×	
Tselepis	✓	✓	×	×	×	×	×	×	×	×	×	
Tiwari and Sodha I	✓	✓	×	✓	✓	✓	×	×	×	×	×	p, T_b, U_t,U_T
Tiwari and Sodha II	✓	✓	×	✓	✓	✓	×	×	×	✓	×	p, T_b, U_t, U_T
Almonacid	✓	✓	✓	×	×	×	×	×	×	×	×	d_1,d_2
Markvart	✓	✓	✓	×	×	×	×	×	×	×	×	
Muzathik	✓	✓	✓	×	×	×	×	×	×	×	×	
Akyuz *et al.*	✓	✓	✓	×	×	×	×	×	×	×	×	
NOCT-1p model	✓	✓	✓	×	×	×	✓	✓	✓	×	×	a,$V_{w,\ NOCT}$
NOCT-2p model	✓	✓	✓	×	×	×	✓	✓	✓	×	×	b, c, $V_{w,\ NOCT}$
ISFOC method	✓	×	×	✓	×	×	×	×	×	×	×	T_b, Cg, L_i, λ_i
Faiman	✓	✓	✓	×	×	×	×	×	×	×	×	U_0, U_1
Skoplaki and Palyvos	✓	✓	✓	×	×	×	×	×	×	×	×	
Skoplaki *et al.* I	✓	✓	✓	×	×	×	×	×	×	×	×	
Duffie and Beckman I	✓	✓	✓	✓	✓	✓	✓	✓	✓	×	×	
Skoplaki *et al.* II	✓	✓	✓	✓	✓	✓	✓	✓	✓	✓	×	h, h_{NOCT}, T_{STC}
Chenni *et al.*	✓	✓	✓	×	×	×	×	×	×	×	×	
Sandia's model	✓	✓	✓	×	×	×	×	×	×	×	×	G_{ref}, e, a, b
Kurtz *et al.*	✓	✓	✓	×	×	×	×	×	×	×	×	
Hornung *et al.*	✓	✓	✓	×	×	×	×	×	×	×	×	m, V_{w0}, c
Coskun *et al.*	✓	✓	✓	×	×	×	×	×	×	×	×	
Duffie and Beckman II	✓	✓	×	✓	✓	×	✓	✓	✓	✓	×	T_{STC}
Mattei	✓	✓	✓	✓	✓	✓	×	×	×	✓	✓	T_{STC}

Solar irradiance, ambient temperature, and wind speed were identified as the most influential parameters, being considered in 100%, 93.9%, and 54.5% of the analyzed models, respectively. These are followed by electrical efficiency (33.3%), solar absorptance (30.3%), and glass transmittance (24.2%). The primary objective of the present work is to estimate the amount of electricity that a standard photovoltaic panel can generate in Boali, thereby assessing its potential contribution to local electrification.

2. Methodology

2.1. Presentation of the study site

Figure 2, which illustrates the photovoltaic potential of the Central African Republic, indicates that the country receives between 4 and 4.8 kWh/day and between 1,461 and 1,753 kWh/year of solar energy that could be harnessed for electricity generation.

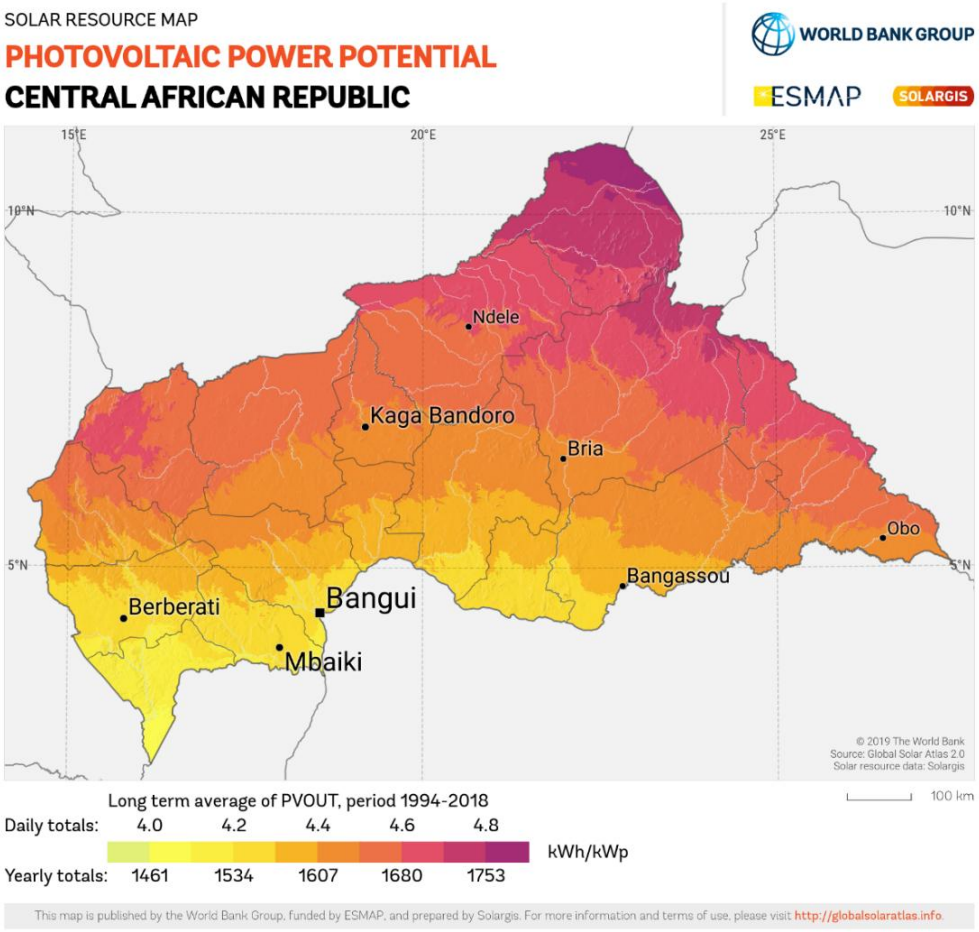

Figure 2 : Average daily and annual PV energy potential in the Central African Republic [29].

The present study was conducted in the town of Boali, located in the Central African Republic. Boali serves as the capital of the Ombella-M'Poko Prefecture, which covers an area of 28,710 km². The town is situated approximately 95 km north-west of Bangui, at an average elevation of 364 m (1,194 ft). Its geographical coordinates are 4°48′00″ N latitude and 18°07′00″ E longitude [30,31]. Figure 3 illustrates the location of the town of Boali [29].

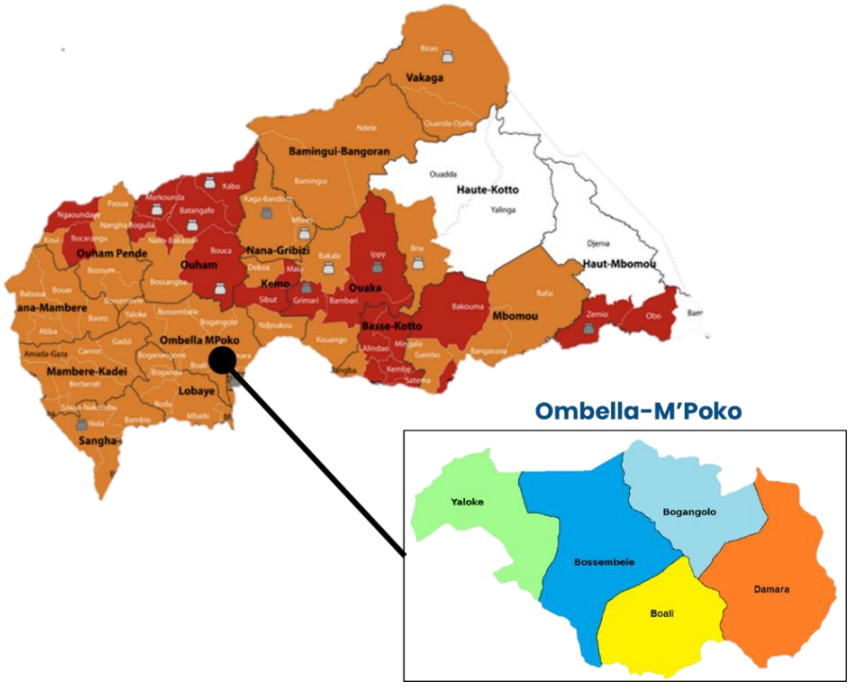

Figure 3 : Geographical location of the study site [31,32]

It is apparent that Boali is situated within a region of the map where the color shifts towards dark orange to red, indicative of elevated PV production values. According to the legend depicted in Figure 2, the region in question exhibits an average daily potential ranging from 4.4 to 4.6 kWh/kWp, with slightly higher values recorded in specific locations (see red/magenta zone). This level of potential is excellent for photovoltaic production and places it among the most favored regions in the CAR, and indeed on the African continent. In terms of annual consumption, the figure is approximately 1 607 to 1 680 kWh/kWp per year. From a climatic point of view, Boali is located within the Sudano-Guinean zone and exhibits a dry winter savannah climate (Aw) according to the Köppen-Geiger classification. Notably, substantial precipitation has been documented, even during the most arid phases of the year. The mean annual temperature in Boali is 25.9°C, with mean annual rainfall varying between 54.6 and 62.4 in. [33], [34].

2.2. Sources of data

In order to assess the photovoltaic solar potential of the town of Boali, relevant meteorological data were first collected. These included records of solar irradiance, ambient temperature, and wind speed. Owing to the absence of an official in-situ meteorological database for the study area within the country's relevant institutions, satellite-based datasets were adopted as reliable alternatives. The SolarGIS tool was used in conjunction with hourly meteorological data retrieved from the NASA POWER database (https://power.larc.nasa.gov/data-access-viewer/). The dataset covered the period from 1 January to 31 December 2024. The hourly values were subsequently extracted and processed using Microsoft Excel to compute daily and monthly averages.

2.3. Model used

The operating temperature of the photovoltaic (PV) module was determined using the empirical model proposed by Skoplaki et al. [35], expressed as follow [35]:

$$T_m = T_a + \omega\left(\frac{0.32}{8.91 + 2V}\right)G \qquad (3)$$

In this equation, T_m and T_a represent the module temperature and the ambient temperature, respectively; ω is the mounting coefficient (1.0 for a free-standing rack and 2.4 for an integrated façade), VVV is the wind speed (m/s), and GGG is the solar irradiance incident on the PV module.

Once the module temperature has been determined, the expected DC power output is calculated using equation (4) [35]:

$$P = \eta AG[1 - \beta(T_a - T_s)] \qquad (4)$$

In In this equation, A is the surface area of the module (m²), η is its nominal efficiency, β is the temperature coefficient, and T is the standard temperature (25 °C).

2.4. Panel characteristics

According to the Hello Watt website [36], three photovoltaic solar panels stand out in 2025 for their excellent cost-performance ratio: the FLASH 500 Half-Cut Glass-Glass TopCon from DualSun, the DM500M10RT-B60HBT from DMEGC Solar, and the Performance 7 from SunPower. These technologies share several common features, including a dual-glass structure, bifacial operation, and the use of TOPCon-type cells. The final selection in this study was based on the assumption that this model offers the highest efficiency, a factor that is particularly relevant in the context of the present estimations. Its main characteristics are summarized in Table 2.

Table 2 : Characteristics of the panel chosen to estimate electricity production [36], [37]

Name	FLASH 500 Half-Cut Glass-Glass TopCon
Manufacturer	Dualsun
Conception	France
Manufacturing	China
Rated power (Wc)	500
Yield (%)	22.61
Length (mm)	1 950
Width (mm)	1 134
Surface (m²)	2.2113
Temperature coefficient (% /°C)	-0.31
Nominal Module Operating Temperature (NMOT) (°C)	45± 2

2.5. Computation steps

As illustrated in Figure 4, the methodology used to estimate the energy production of the photovoltaic system is based on climatic data. For each step of the process, the tools or data sources are indicated in the left-hand column, the corresponding processing steps are described in the central column, and the resulting outputs or data are presented in the right-hand column.

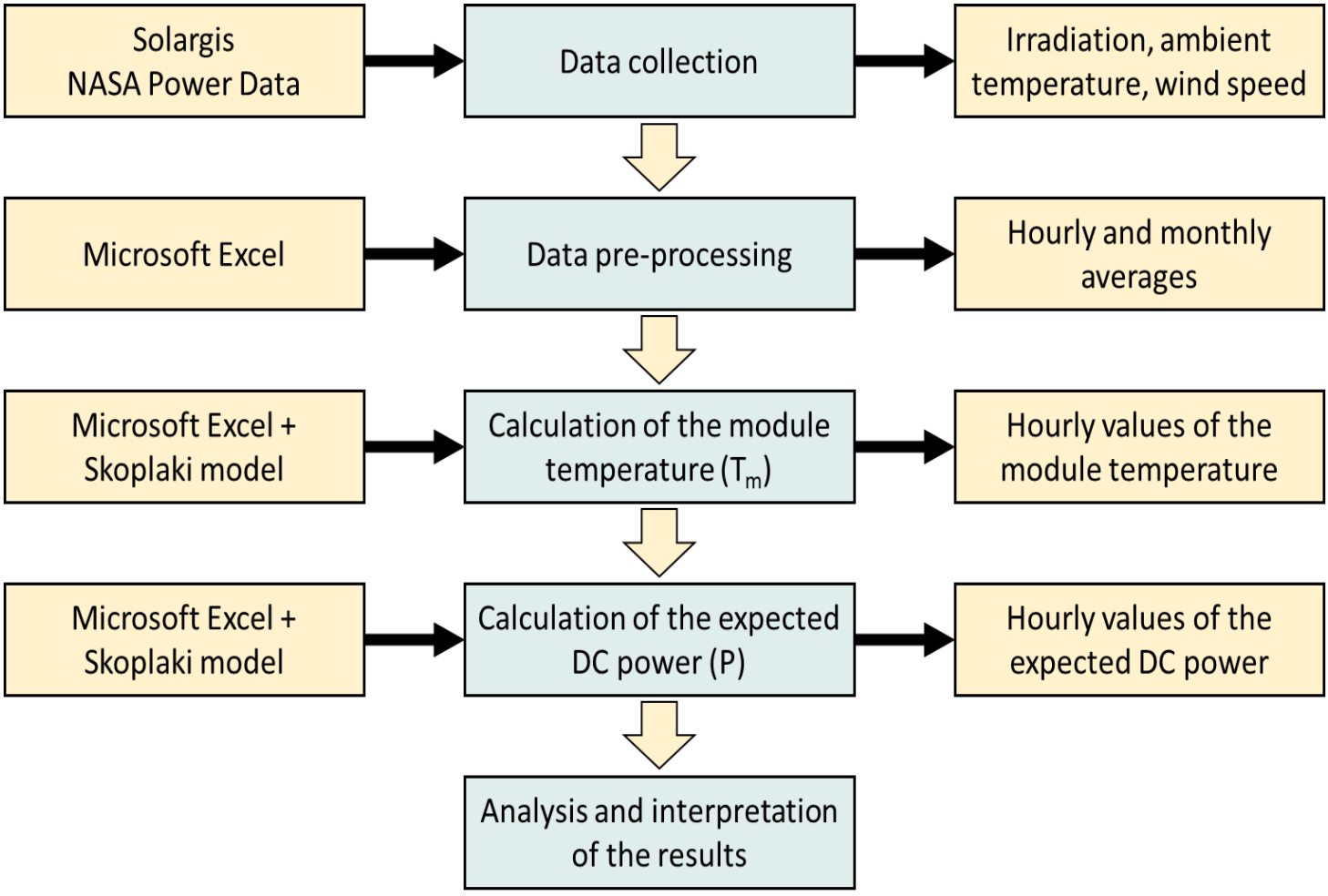

Figure 4 : Diagram of the methodology used to estimate energy production

3. Results and discussion

Figure 5 illustrates the seasonal variations in sunrise and sunset times, as well as in day length and night duration, at the study site.

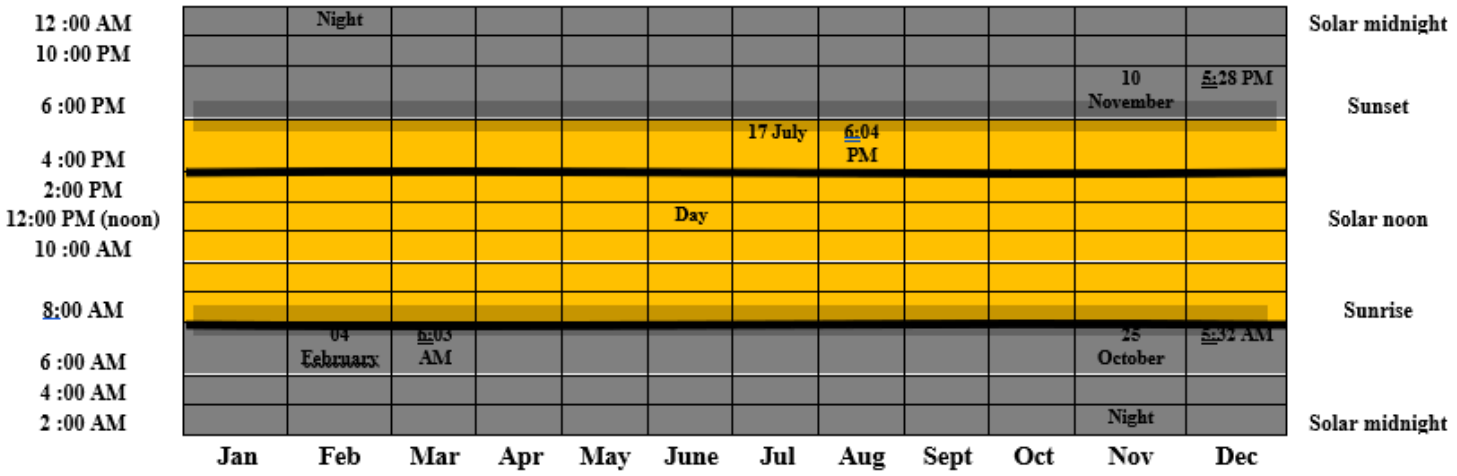

Figure 5 : Sunrise and sunset times throughout the year in Boali, showing seasonal variations in day length.

The black lines, extending vertically across the diagram, represent the sequence of solar events, beginning with the previous solar midnight, followed by sunrise, solar noon, and sunset, and ending with the subsequent solar midnight. The colored bands, ranging from yellow to grey, indicate daytime, the different phases of twilight (civil, nautical, and astronomical), and night. The sun rises before 6:00 a.m. between April and November. The earliest sunrise is recorded at 05:32 on 25 October, while the latest occurs at 06:03 on 4 February. Similarly, the earliest sunset is observed at 17:28 on 10 November, whereas the latest takes place after 18:04 on 17 July.

The figure reveals only minor variations in sunrise and sunset times over the course of the year, indicating that day length remains relatively stable. This regularity reflects Boali's proximity to the equator and suggests that the daily solar energy input does not vary significantly between seasons. Such stability is particularly advantageous for photovoltaic system design, as solar availability remains relatively uniform, enabling predictable energy production without the need for seasonal tilt adjustments or solar tracking systems.

Figure 6 illustrates the daily duration of sunshine (black line), together with the twilight phases (colored bands) and full night (grey), for the study location over the course of the year.

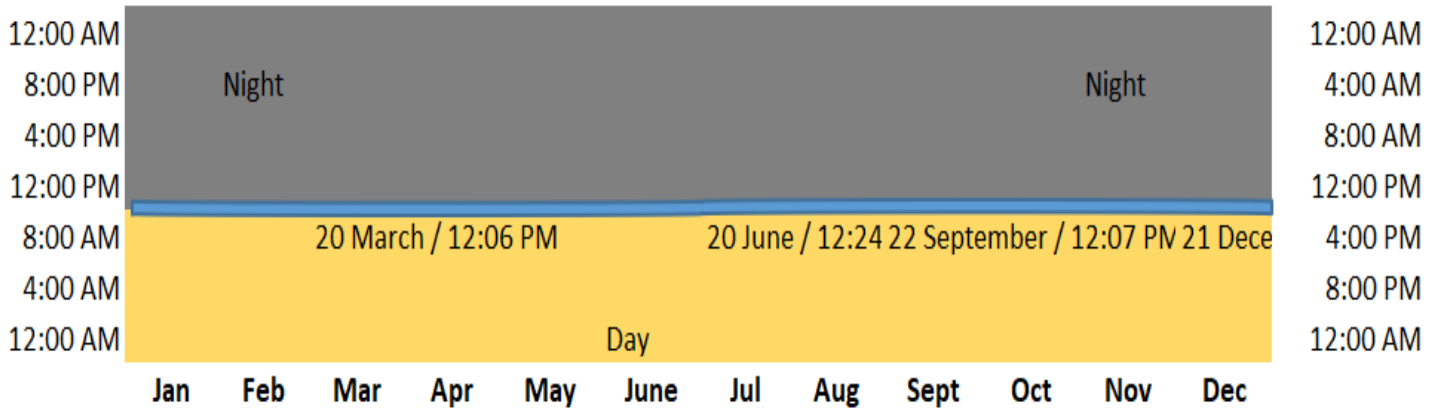

Figure 6 : Daily sunshine duration in Boali across the year.

The color-coding system used in this study extends from bottom to top (yellow to grey), with each color representing a specific phase of the day. These phases include daytime, the different stages of twilight (civil, nautical, and

astronomical), and full night. The graph indicates that the longest duration of sunshine reaches 12 hours and 24 minutes, occurring on 20 June, while the shortest duration is 11 hours and 51 minutes, occurring on 21 December, which correspond respectively to the summer and winter solstices. The figure also shows that Boali receives more than 11 hours of sunshine per day even during the least favorable months. This confirms the site's excellent solar exposure and its high suitability for continuous photovoltaic energy production.

Figure 7 illustrates the annual evolution of solar elevation in Boali. This graphical representation enables the identification of periods of the year and times of day during which solar radiation is at its highest, which is essential for optimal panel orientation and system design. The black lines correspond to constant solar elevation angles, that is, the angle of the sun above the horizon expressed in degrees. The colored background represents the solar azimuth, while the lighter-colored areas at the boundaries of the cardinal directions indicate the intermediate orientations (north-east, south-east, south-west, and north-west).

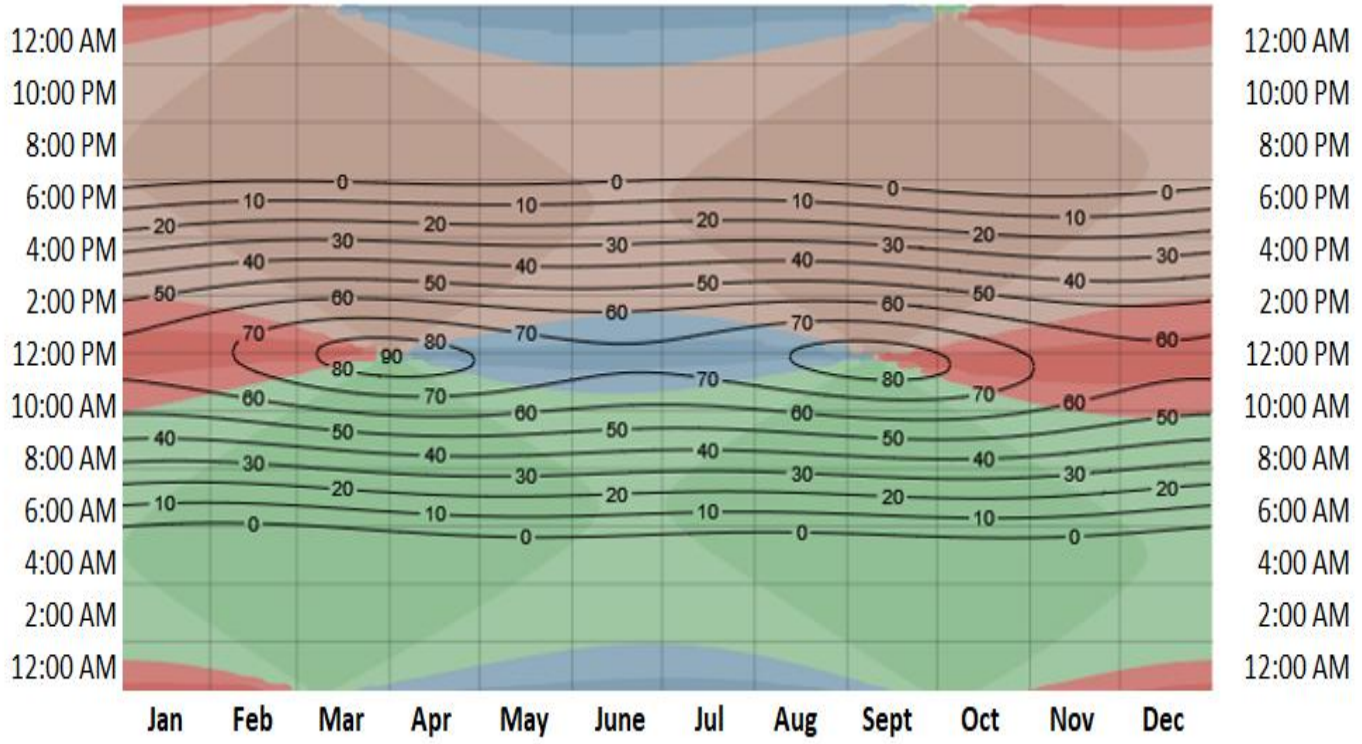

Figure 7: Annual variation of solar elevation and azimuth in Boali.

The maximum solar elevation reaches approximately 90° around solar noon, particularly during the equinoxes (March and September), thereby confirming Boali's proximity to the equator (latitude ≈ 4.8° N). Such high solar angles imply that the incoming radiation is almost perpendicular to a horizontal surface at midday. The town's geographical position results in relatively consistent solar exposure throughout the year, characterized by nearly symmetrical day lengths.

During the solstices (June and December), although the maximum solar elevation is slightly reduced (approximately 70–80°), this variation remains moderate, thus confirming the limited seasonal influence on daily global irradiance. This indicates that photovoltaic panels in Boali may be installed with a very low tilt angle (about 5–10°), or even in a horizontal position, while still maintaining a high energy yield throughout the year. Therefore, the persistently high solar elevation constitutes a major advantage for the design of cost-effective PV systems requiring minimal tilt adjustment.

The combination of the three aforementioned results suggests that the optimal inclination of solar panels can remain remarkably low (between 5° and 10°), or even 0° in the case of flat installations, given the consistently high position of the sun around midday. It is also noteworthy that a strict southward orientation (in the Northern Hemisphere) is not a prerequisite for optimal performance, since systems with a fixed orientation can still exhibit satisfactory efficiency.

Table 3 presents the monthly average values of global and diffuse solar irradiance on a horizontal plane, together with other meteorological parameters relevant to the evaluation of solar potential in Boali.

Table 3 : Average monthly values for irradiation and other meteorological parameters

N°	Month	Temperature [°C]	Wind speed [m/s]	Linke Turbidity [-]	Relative Humidity [%]
1	January	26.10	1.40	5.40	64.80
2	February	27.00	1.50	5.80	61.00
3	March	27.50	1.80	5.70	69.70
4	April	26.50	1.70	4.20	78.50
5	May	26.50	1.60	3.60	78.30
6	June	25.30	1.40	4.10	83.00
7	July	25.20	1.30	3.80	83.20
8	August	25.00	1.40	3.50	84.60
9	September	24.90	1.40	3.40	83.00
10	October	25.00	1.30	3.60	83.10
11	November	25.30	1.20	4.10	81.30
12	December	24.40	1.10	5.10	69.90
Average		25.73	1.43	4.36	76.70

Figure 8 illustrates the monthly evolution of global and diffuse solar irradiation on a horizontal surface in Boali. The results derived from the climatic data for the town of Boali reveal a substantial solar potential, with an average global irradiation of approximately 150.63 kWh/m²/month, corresponding to nearly 1,800 kWh/m²/year. This value falls within a favourable range for the deployment of high-efficiency photovoltaic (PV) systems. On the other hand, the diffuse component accounts for a significant proportion of the total irradiance (around 50%), particularly during the rainy season (June to October), indicating the influence of cloud cover, high humidity, and increased aerosol concentrations. Consequently, the effect of diffuse radiation on panel performance must be taken into consideration, notably through the adoption of photovoltaic technologies adapted to diffuse-light conditions.

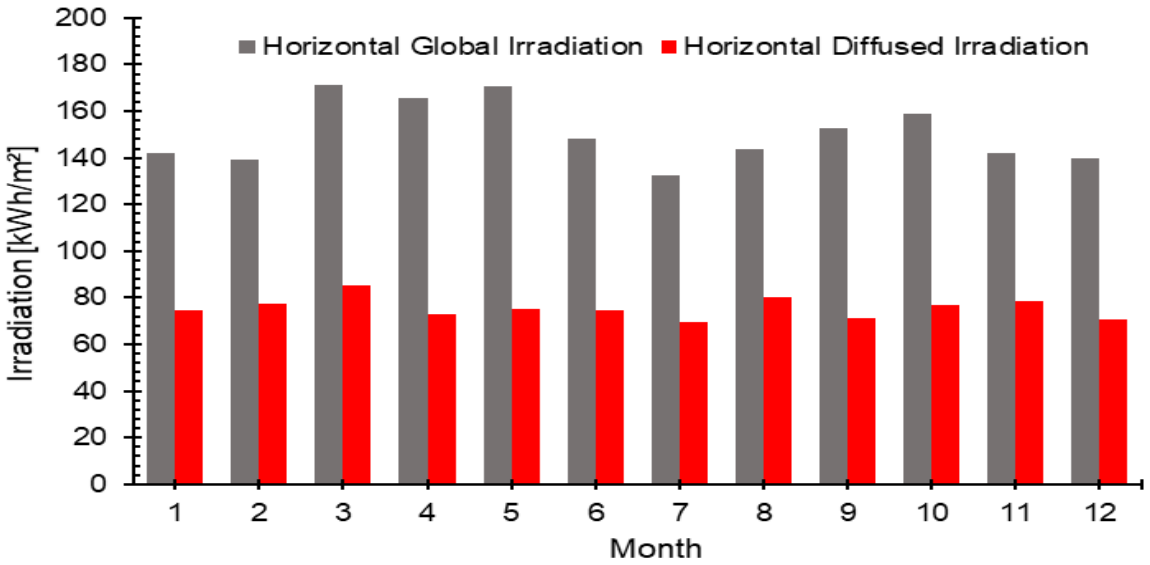

Figure 8: Monthly evolutions in global and diffuse solar irradiation on a horizontal plane in Boali.

The observed seasonal pattern reflects the typical alternation between dry and wet periods characteristic of the Sudano-Guinean climate. During the rainy months, enhanced cloud cover increases the diffuse fraction of solar radiation while slightly reducing the total amount of energy received. Nevertheless, the overall annual solar potential

remains high, thereby confirming Boali's favourable position for photovoltaic power generation. Moderate seasonal variability is nonetheless recorded, with global irradiation decreasing by approximately 22% between March (a peak value of 171.5 kWh/m²) and July (132.3 kWh/m²). This reduction is largely attributable to the rainy season, which is characterized by relative humidity levels exceeding 80% and elevated atmospheric turbidity. Indeed, cloud cover strongly attenuates direct normal irradiance (DNI) while increasing the diffuse fraction of the radiation field; consequently, the total global horizontal irradiance (GHI) declines during this period. This pattern has been widely documented in similar West and Central African contexts and is commonly cited as an explanation for mid-year minima in tropical solar irradiance records [38].

Figure 9 presents the hourly average profile of global irradiance over the entire year on one side, and the hourly average wind speed at 10 m above ground on the other. The values are color-coded, allowing for a clear visual identification of periods characterized by high and low resource availability.

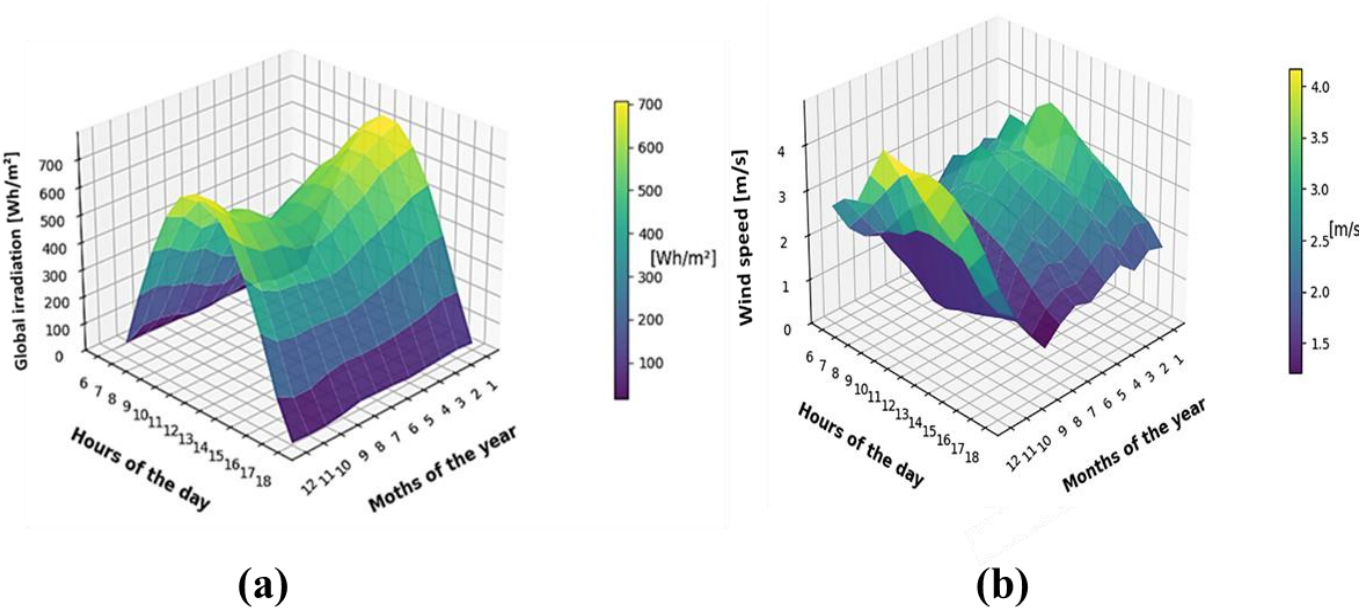

Figure 9: Hourly average global irradiance profile (Wh/m²) over the entire year (a) and hourly average wind speed profile (m/s) at 10 m above ground (b).

An hourly analysis of solar irradiance indicates that peak values are consistently observed between 10:00 a.m. and 2:00 p.m., with levels exceeding 700 Wh/m² during the dry season (January to March and November to December). In contrast, the months of June and July exhibit a marked decline in irradiance, with minimum values falling below 550 Wh/m². This reduction is indicative of increased cloud cover and elevated humidity levels, which were recorded during the same period (with average humidity exceeding 83%).

The mean wind speed measured at a height of 10 m remains relatively low throughout the year, fluctuating between 1.2 m/s and 3.8 m/s. The highest values are generally observed between 10:00 a.m. and 12:00 p.m. This phenomenon is of particular interest with regard to the passive cooling of photovoltaic modules.

Furthermore, the hourly ambient temperature profiles (Figure 10) reveal a pronounced increase in temperature between 11:00 a.m. and 3:00 p.m., a time interval that coincides with peak solar irradiance. The highest temperatures, recorded mainly between February and April, commonly range between 32°C and 33°C, representing a critical period from a thermal perspective.

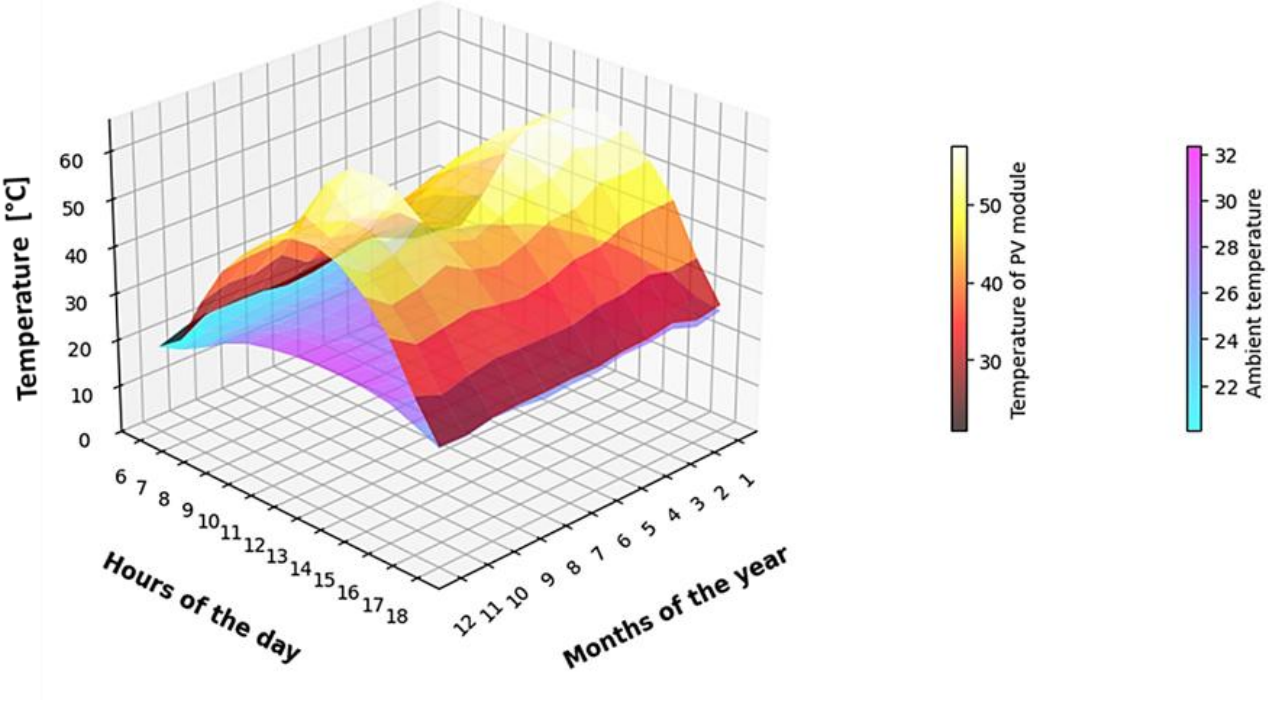

Figure 10: Hourly average ambient temperature profile [°C] at 2 m above ground throughout the year and hourly temperature profile of PV module [°C] throughout the year.

In accordance with the solar irradiance profile, the highest module temperatures are recorded between 11:00 a.m. and 2:00 p.m. During this time interval, temperatures frequently exceed 50°C in all months, reaching peak values of approximately 58.60°C (12:00–13:00, December) and 60.51°C (11:00–12:00, September). These temperatures are substantially higher than the Standard Test Condition (STC) temperature of 25°C, at which the rated power of the modules is defined, and exceed the operating temperature range recommended by the manufacturer, i.e. 45 ± 2°C. The temperature of the PV modules is primarily governed by incident solar irradiance and convective heat transfer. During the rainy season, reduced irradiance generally contributes to lower module temperatures; however, higher humidity levels and reduced wind speeds during certain periods may partially offset this cooling effect. In the present case, the decrease in incident energy during the rainy months outweighs the modest efficiency gains associated with lower operating temperatures. Consequently, overall power production declines during this period.
This thermal behavior exerts a direct influence on photovoltaic performance, particularly considering the negative temperature coefficient of conventional crystalline silicon panels (approximately –0.4 %/°C). This observation is fully consistent with previously reported empirical measurements and modelling studies that have examined the combined effects of temperature and irradiance on PV system performance [9,10].

Table 4: Estimated hourly power output of a photovoltaic module for each month of the year

Hour	Jan	Feb	Mar	Apr	May	Jun	Jul	Aug	Sep	Oct	Nov	Dec
5 - 6				0.063	0.830	0.518	0.134	0.056	0.561	1.555	0.585	
6 - 7	17.354	14.081	16.004	30.231	34.628	28.931	23.346	22.899	36.910	45.099	45.218	25.617
7 - 8	111.457	98.467	95.720	107.769	104.673	90.735	81.756	91.161	113.670	121.899	136.059	131.411
8 - 9	216.600	199.422	185.399	193.294	180.897	161.593	149.938	165.382	199.719	204.073	227.150	232.708
9 - 10	308.091	289.777	267.838	268.492	248.225	225.403	207.964	233.069	270.205	267.252	303.231	316.593
10 - 11	369.736	350.279	327.517	319.331	292.507	271.342	251.428	277.631	313.739	302.054	348.688	372.673
11 - 12	398.622	381.427	358.459	335.378	311.449	286.938	267.353	287.982	326.071	324.978	363.435	393.382
12 - 13	395.662	382.177	360.759	333.448	312.701	285.098	269.549	279.074	317.841	319.315	347.252	383.754
13 - 14	358.327	347.701	334.722	301.346	283.265	256.826	243.646	250.133	279.102	277.998	301.763	341.103
14 - 15	291.533	283.220	263.082	243.622	229.398	206.540	194.829	201.621	213.570	215.190	230.398	271.056
15 - 16	201.124	197.837	178.164	166.941	155.191	143.221	134.598	140.350	143.540	141.055	146.634	179.611

16 - 17	98.981	100.836	89.063	81.229	75.672	72.269	71.647	74.307	68.766	56.175	55.418	73.472
17 - 18	12.831	15.829	13.439	11.377	8.856	11.440	12.462	13.835	6.531	1.739	1.421	3.084
Total	2780.318	2661.054	2490.165	2392.459	2237.463	2040.337	1908.518	2037.443	2289.666	2276.826	2506.667	2724.464

The graphs presented in Figure 11 illustrate how the power output of a photovoltaic module varies throughout both the year and the day. In Figure 11a, each colored curve represents a specific time interval, and the x-axis (Months) extends from 1 to 12, corresponding to January through December. In Figure 11b, each colored curve represents a specific month of the year, while the x-axis represents the hours of the day, ranging from 06:00 to 18:00. The y-axis depicts the direct current (DC) power output of the photovoltaic module, expressed in watts (W).

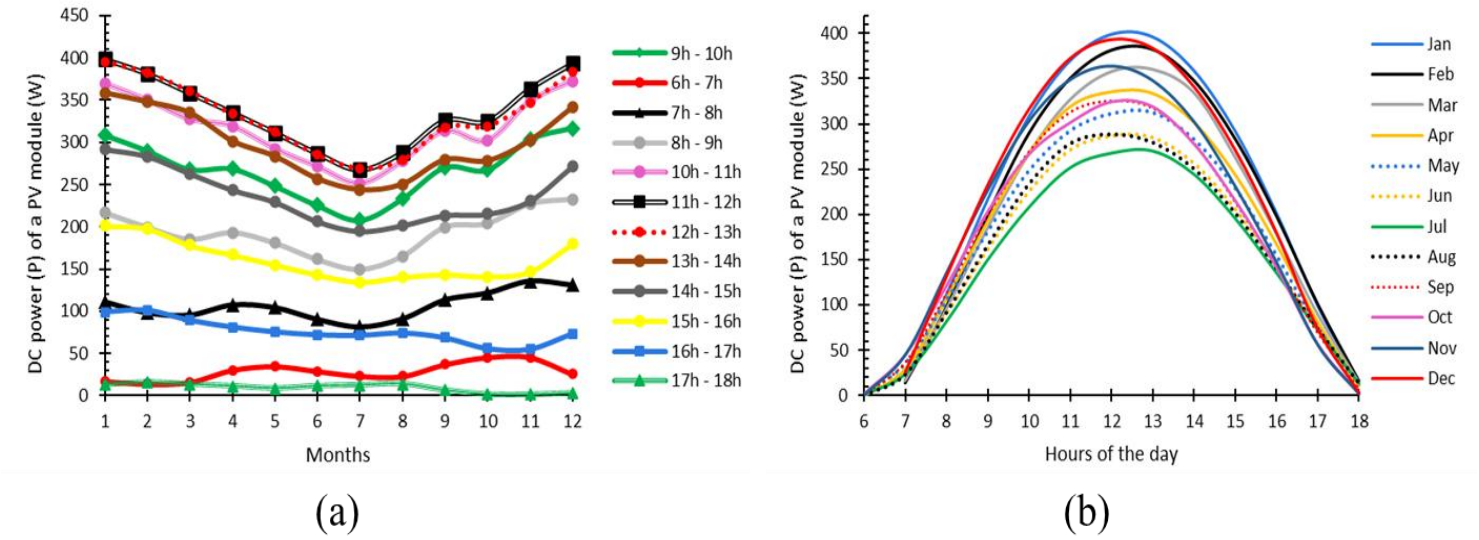

Figure 11 : Seasonal and diurnal variation of photovoltaic power output.

The energy production profile exhibits a characteristic bell-shaped curve across all months, typical of the diurnal pattern of solar radiation. Power output increases markedly after 06:00, reaches a maximum between 12:00 and 13:00, and then gradually decreases until 18:00. The highest power peak is consistently observed during the 12:00–13:00 interval for all months, corresponding to the period when the sun reaches its greatest elevation and solar irradiance is at its maximum. The time window between approximately 11:00 and 13:00 therefore represents the most critical period in terms of power generation.

In 2022, the Central African Republic recorded a particularly low per-capita electricity consumption, estimated at 27 kWh per person per year [33]. Using the 500 Wp panel considered in this study, the estimated annual energy production is approximately 28.3 kWh per panel. This value is of the same order of magnitude as the reported per-capita electricity consumption in the Central African Republic (≈ 27 kWh per person per year), highlighting the relative significance of the photovoltaic resource in this context. However, it should be emphasized that this comparison is purely indicative: equating one panel to one person represents an oversimplification, as it does not account for temporal mismatches, storage requirements, or distribution losses.

Comparisons with regional studies, including investigations of photovoltaic potential and small-scale PV systems in Cameroon conducted by Dongmo et al., as well as techno-economic analyses of rural PV systems in Chad by Hassane et al., indicate that the solar resource in Boali and the simulated annual output of a 500 Wp panel are consistent with expectations for comparable tropical environments [39,40].

Finally, it is important to note that the present study is based on satellite-derived meteorological datasets (SolarGIS and NASA POWER). While such products are indispensable in data-scarce regions, they are subject to spatially variable biases and root-mean-square errors. Independent validation studies have shown that different datasets (SolarGIS, NASA POWER, Meteonorm, and various reanalysis products) exhibit varying levels of accuracy and bias, with SolarGIS generally demonstrating relatively low bias among currently available sources [41].

4.Conclusion

This study provides the first localized assessment of the photovoltaic potential of the town of Boali (Central African Republic), based on hourly satellite-derived climatic data and the Skoplaki model. The results indicate that Boali benefits from significant solar resources, with an estimated annual energy production of approximately 28 kWh per 500 Wp panel. This value is comparable to the current average per-capita electricity consumption in the country, thereby highlighting the potential contribution of small-scale photovoltaic systems to rural electrification. The findings further confirm that Boali presents favorable conditions to serve as a pilot site for decentralized solar electrification projects. Future work should incorporate in-situ measurements in order to validate the satellite-based data and should also investigate hybrid configurations and energy storage solutions to enhance the reliability and long-term sustainability of the energy supply.

Financial supports

No funds, grants, or other financial support was received for conducting this study or for preparing this manuscript.

Competing Interests

The authors declare that they have no known competing financial interests or personal relationships that could have appeared to influence the work reported in this paper.

References

1. Olong, G., Eke, S., Boum, A., Manyol, M., Biboum, A., & Mouangue, R. (2023). *Assessment of the conventional energy potential in Cameroon: The use of wind, small hydro, and solar technologies as alternative solutions*. International Journal of Renewable Energy Research, 13(1), 79–88.
2. Sokona, Y., Mulugetta, Y., & Gujba, H. (2012). *Widening energy access in Africa: Towards energy transition*. Energy Policy, 47, 3–10. https://doi.org/10.1016/j.enpol.2012.03.040
3. Ngbara Touafio, J. F., Sanda, O., Malenguinza, S., M'Boliguipa, J., & Mouangue, R. M. (2020). *Analysis of a wind turbine project in the city of Bouar (Central African Republic)*. Scientific African, 8, e00354. https://doi.org/10.1016/j.sciaf.2020.e00354
4. Ngbara Touafio, J. F., Malenguiza, S., Oumarou, S., Kazet, M. Y., & Mouangue, R. M. (2019). *Statistical analysis and elaboration of the wind potential map of the city of Bangui (Central African Republic)*. Renewable Energy Focus, 29, 1–13. https://doi.org/10.1016/j.ref.2019.01.001
5. Radio Ndeke Luka. (2025). *Centrafrique : la capacité de l'Enerca augmente de 15 mégawatts supplémentaires grâce au champ solaire de Sakaï*. Retrieved May 26, 2025, from https://www.radiondekeluka.org/40233-centrafrique-la-capacite-de-l-enerca-augmente-de-15-megawatts-supplementaires-grace-au-champ-solaire-de-sakai
6. World Bank Group. (2023). *With the support of the World Bank, a new solar park in the Central African Republic expands access to clean energy*. Retrieved May 26, 2025, from https://www.worldbank.org/en/news/press-release/2023/11/17/with-the-support-of-the-world-bank-a-new-solar-park-in-the-central-african-republic-expands-access-to-clean-energy
7. World Bank Group. (2025). *World Development Indicators*. Retrieved May 26, 2025, from https://databank.worldbank.org/source/world-development-indicators
8. Fumtchum, G., Ekoe Akata, A. M., Mouangue, R., & Dakyo, B. (2023). *Predicting the efficiency of solar photovoltaic energy injection in a localized subtropical grid by modelling actual generation trend curves: Case study of Douala*. International Journal of Renewable Energy Research, 13(4), 1614–1620.
9. Skoplaki, E., & Palyvos, J. A. (2009). *On the temperature dependence of photovoltaic module electrical performance: A review of efficiency/power correlations*. Solar Energy, 83(5), 614–624. https://doi.org/10.1016/j.solener.2008.10.008

10. Skoplaki, E., Boudouvis, A., & Palyvos, J. (2008). *A simple correlation for the operating temperature of photovoltaic modules of arbitrary mounting*. Solar Energy Materials and Solar Cells, 92, 1393–1402. https://doi.org/10.1016/J.SOLMAT.2008.05.016
11. Trinuruk, P., Sorapipatana, C., & Chenvidhya, D. (2009). *Estimating operating cell temperature of BIPV modules in Thailand*. Renewable Energy, 34, 2515–2523. https://doi.org/10.1016/J.RENENE.2009.02.027
12. Aoun, N. (2019). *Outdoor testing of free standing PV module temperature under desert climate: A comparative study*. International Journal of Ambient Energy, 42, 1484–1491. https://doi.org/10.1080/01430750.2019.1611640
13. Aoun, N. (2022). *Methodology for predicting the PV module temperature based on actual and estimated weather data*. Energy Conversion and Management: X. https://doi.org/10.1016/j.ecmx.2022.100182
14. Bailek, N., Bouchouicha, K., Hassan, M. A., Slimani, A., & Jamil, B. (2020). *Implicit regression-based correlations to predict the back temperature of PV modules in the arid region of south Algeria*. Renewable Energy, 156, 57–67. https://doi.org/10.1016/j.renene.2020.04.073
15. Kaplani, E., & Kaplanis, S. (2014). *Thermal modelling and experimental assessment of the dependence of PV module temperature on wind velocity and direction, module orientation and inclination*. Solar Energy, 107, 443–460. https://doi.org/10.1016/J.SOLENER.2014.05.037
16. De Souza, A., Aristone, F., Ferrari, L. F., & Rezende, R. (2016). *Modelagem da temperatura do módulo de células fotovoltaicas em função da temperatura ambiente, velocidade dos ventos e irradiância*. https://doi.org/10.5380/RBER.V5I4.46453
17. Aly, S., Ahzi, S., Barth, N., & Abdallah, A. (2018). *Using energy balance method to study the thermal behavior of PV panels under time-varying field conditions*. Energy Conversion and Management. https://doi.org/10.1016/J.ENCONMAN.2018.09.007
18. Perović, B., Klimenta, D., Jevtić, M., & Milovanović, M. (2019). *A transient thermal model for flat-plate photovoltaic systems and its experimental validation*. Elektronika ir Elektrotechnika. https://doi.org/10.5755/J01.EIE.25.2.23203
19. Barry, J., et al. (2020). *Dynamic model of photovoltaic module temperature as a function of atmospheric conditions*. Advances in Science and Research, 17, 165–173. https://doi.org/10.5194/asr-17-165-2020
20. Frid, S., Mordynskii, A. V., & Avezova, N. R. (2023). *The influence of a photovoltaic module thermal model choice on the error of calculating the module performance*. Applied Solar Energy. https://doi.org/10.3103/s0003701x23600996
21. Coskun, C., Koçyiğit, N., & Oktay, Z. (2016). *Estimation of PV module surface temperature using artificial neural networks*. Muğla Journal of Science and Technology, 2, 15–18. https://doi.org/10.22531/MUGLAJSCI.283611
22. Serrano-Luján, L., Toledo, C., Colmenar, J., Abad, J., & Urbina, A. (2022). *Accurate thermal prediction model for building-integrated photovoltaics systems using guided artificial intelligence algorithms*. Applied Energy. https://doi.org/10.1016/j.apenergy.2022.119015
23. Xiaojian, D., Shen, J., He, G.-X., Ma, Z., & He, Y.-J. (2021). *A general radial basis function neural network assisted hybrid modeling method for photovoltaic cell operating temperature prediction*. Energy, 234, 121212. https://doi.org/10.1016/J.ENERGY.2021.121212
24. Orazioa, D. M., Pernab, C. D., & Giuseppea, E. D. (2014). *Performance assessment of different roof integrated photovoltaic modules under Mediterranean climate*. Energy Procedia, 42, 183–192. https://doi.org/10.1016/J.EGYPRO.2013.11.018
25. Martín-Chivelet, N., Polo, J., Sanz-Saiz, C., Benítez, L. T. N., Alonso-Abella, M., & Cuenca, J. (2022). *Assessment of PV module temperature models for building-integrated photovoltaics (BIPV)*. Sustainability. https://doi.org/10.3390/su14031500
26. Assoa, Y., Gaillard, L., Ménézo, C., Negri, N., & Sauzedde, F. (2018). *Dynamic prediction of a building-integrated photovoltaic system thermal behaviour*. Applied Energy, 214, 73–82. https://doi.org/10.1016/J.APENERGY.2018.01.078

27. Assoa, Y., Valencia-Caballero, D., Rico, E., del Caño, T., & Furtado, J. V. (2023). *Performance of a large size photovoltaic module for façade integration*. Renewable Energy. https://doi.org/10.1016/j.renene.2023.04.087
28. De O. Santos, L., De Carvalho, P. C. M., & De O. C. Filho, C. (2022). *Photovoltaic cell operating temperature models: A review of correlations and parameters*. IEEE Journal of Photovoltaics, 12(1), 179–190. https://doi.org/10.1109/JPHOTOV.2021.3113156
29. World Bank Group, ESMAP, & Solargis. (2025). *Global Solar Atlas*. Retrieved May 24, 2025, from https://globalsolaratlas.info/download/central-african-republic
30. DB-City. (2025). *Boali*. Retrieved May 24, 2025, from https://fr.db-city.com/R%C3%A9publique-centrafricaine--Ombella-Mpoko--Boali
31. Gifex. (2025). *Carte de la préfecture de l'Ombella-M'Poko*. Retrieved May 24, 2025, from https://gifex.com/fr/fichier/carte-de-la-prefecture-de-l-ombella-mpoko/
32. FAO. (2021). *République centrafricaine : Moyens d'existence agricoles et sécurité alimentaire dans le cadre de la COVID-19*. FAO, Rome. https://doi.org/10.4060/cb5267fr
33. Le planificateur A-contresens. (2025). *Quand partir à Boali en République centrafricaine ?* Retrieved May 24, 2025, from https://planificateur.a-contresens.net/afrique/republique_centrafricaine/ouham/boali/2388719.html
34. Dongbada-Tambano, M. T., Foto, B. A. E., & Mandjeka, J.-C. A. (2020). *Identification et priorisation des technologies aux fins d'adaptation aux changements*.
35. Skoplaki, E., Boudouvis, A. G., & Palyvos, J. A. (2008). *A simple correlation for the operating temperature of photovoltaic modules of arbitrary mounting*. Solar Energy Materials and Solar Cells, 92(11), 1393–1402. https://doi.org/10.1016/j.solmat.2008.05.016
36. Hello Watt. (2025). *[Guide] Installer les meilleurs panneaux solaires en 2025*. Retrieved May 24, 2025, from https://www.hellowatt.fr
37. DualSun. (2023, November 22). *Fiche technique – DualSun Flash TopCon 500*.
38. Niang, S. A. A., Gueye, A., Sarr, A., Diop, D., Goni, S., & Nebon, B. (2023). *Comparative study of available solar potential for six stations of Sahel*. Smart Grid and Renewable Energy, 14(8), 153–167. https://doi.org/10.4236/sgre.2023.148009
39. Dongmo, C. O., Arreyndip, N. A., Tendong, E., Afungchui, D., Daoudi, M., & Ebobenow, J. (2024). *Assessing the performance of a monocrystalline solar panel under different tropical climatic conditions in Cameroon using artificial neural network*. Journal of Renewable and Sustainable Energy, 16(5). https://doi.org/10.1063/5.0225780
40. Hassane, A. I., et al. (2022). *Techno-economic feasibility of a remote PV mini-grid electrification system for five localities in Chad*. International Journal of Sustainable Engineering, 15(1), 177–191. https://doi.org/10.1080/19397038.2022.2101707
41. Pedersen, A. (2024). *Solargis solar resource database validation of satellite-based solar radiation model (customer consultant: The World Bank)*. https://solargis.com